Swift Observations of GRB 050603: An afterglow with a steep late time decay slope

Dirk Grupe[1],
grupe@astro.psu.edu
Peter J. Brown[1], Jay Cummings[2], Bing Zhang[3], Alon Retter[1], David N. Burrows[1], Patricia T. Boyd[2], Milvia Capalbi[4] Neil Gehrels[2] Stephen T. Holland[2,5], Peter Mészáros [1,6], John A. Nousek[1], Jamie A. Kennea[1], Paul O'Brien[7], Julian Osborne[7], Claudio Pagani[1], Judith L. Racusin[1], Peter Roming[1], and Patricia Schady[1,8]

ABSTRACT

We report the results of *Swift* observations of the Gamma Ray Burst GRB 050603. With a V magnitude V=18.2 about 10 hours after the burst the optical afterglow was the brightest so far detected by *Swift* and one of the brightest optical afterglows ever seen. The Burst Alert Telescope (BAT) light curves show three fast-rise-exponential-decay spikes with T_{90}=12s and a fluence of 7.6×10^{-6} ergs cm^{-2} in the 15-150 keV band. With an $E_{\gamma,\rm iso} = 1.26 \times 10^{54}$ ergs it was also one of the most energetic bursts of all times. The *Swift* spacecraft began observing of the afterglow with the narrow-field instruments about 10 hours after the detection of the burst. The burst was bright enough to be detected by the *Swift* UV/Optical telescope (UVOT) for almost 3 days and by the X-ray Telescope (XRT) for a week after the burst. The X-ray light curve shows a rapidly fading afterglow with a decay index α=$1.76^{+0.15}_{-0.07}$. The X-ray energy spectral index was $\beta_{\rm X}$=0.71±0.10 with the column density in agreement with the Galactic value. The spectral analysis does not show an obvious change in the X-ray spectral slope over time. The optical UVOT light curve decays with a slope of α=1.8±0.2. The steepness and the similarity of the optical and X-ray decay rates suggest that the afterglow was observed after the jet break. We estimate a jet opening angle of about 1-2°.

Subject headings: GRBs:individual(GRB 050603)

[1]Department of Astronomy and Astrophysics, Pennsylvania State University, 525 Davey Lab, University Park, PA 16802

[2]NASA Goddard Space Flight Center, Greenbelt, MD 20771

[3]Department of Physics, University of Nevada, Las Vegas, NV 89154

[4]ASI Science Data Center, via G. Galilei, I-00044 Frascati (Roma), Italy

[5]Universities Space Research Association, Seabrook, MD

[6]Department of Physics, Pennsylvania State University, University Park, PA 16802

[7]Department of Physics & Astronomy, University of Leicester, Leicester, LE1 7R, UK

[8]Mullard Space Science Laboratory, Holmbury St. Mary, Dorking, Surrey RH5 6NT, U.K.

1. Introduction

With an isotropic equivalent energy release on the order of $10^{52} - 10^{54}$ ergs, Gamma Ray Bursts (GRBs) are among the most energetic events in the Universe besides the Big Bang. GRBs can be separated into two classes: short and long bursts. Long bursts, with durations longer than 2 seconds (e.g. Kouveliotou et al. 1993) are associated with the collapse of a very massive star and the formation of a black hole (Woosley 1993). Short bursts are thought to be the result of a neutron star (NS) - NS or NS - black hole merger (e.g Eichler et al., 1989; Paczyński 1991). The leading theoretical model for GRBs and their afterglows is the fireball model (see Mészáros & Rees 1997; Sari et

al. 1998; Zhang & Mészáros 2004, and references within) in which the GRB is produced by internal shocks in a relativistic fireball, while the afterglow is produced in external shocks which are created when the fireball encounters the ambient external medium.

The multi-wavelength mission *Swift* (Gehrels et al. 2004) was launched on 2004-November-20 in order to hunt for GRBs. It is in low-Earth orbit at an altitude of 600 kms. The *Swift* observatory is equipped with three telescopes: a) the Burst Alert Telescope (BAT, Barthelmy 2005), b) the X-Ray Telescope (XRT, Burrows et al. 2005b), and c) the UV-Optical Telescope (UVOT, Roming et al. 2005). The BAT is a coded mask experiment and operates in the 15-350 keV energy range. The XRT detector is a copy of the MOS CCDs used on-board XMM (Turner et al. 2001). It operates between 0.3-10 keV in three observing modes, Photon Counting (PC) which is equivalent to the full-frame mode on XMM, Windowed Timing (WT), and Low-Rate Photo-diode mode (LrPD) which is only used for extremely bright sources (Hill et al. 2004). The UVOT is a sister instrument to XMM's Optical Monitor (OM, Mason et al. 2001) and includes a similar set of filters to the OM (Mason et al. 2001; Roming et al. 2005).

As reported by Nousek et al. (2006), *Swift* has observed a general behavior of GRB afterglow X-ray light curves: a fast decay with slope α_1 in the first hundred seconds is followed by a much shallower decay slope α_2. This continues over a span of several thousands of seconds after the burst and is followed by a steeper decay slope α_3 (see also Zhang et al. 2006). The mean decay slopes of the 27 afterglows discussed in Nousek et al. (2006) are: α_1=3.38±1.27, α_2=0.76±0.34, and α_3=1.33±0.32.

In this paper we report the *Swift* observations of GRB 050603. The paper is organized as follows: In §2 we describe the observations and the data reduction and analysis, in §3 we present the results which are then discussed in §4. Throughout the paper decay and energy spectral indices α and β are defined as $F_\nu(t,\nu) \propto (t-t_0)^{-\alpha}\nu^{-\beta}$ with t_0 the trigger time of the burst. Luminosities are calculated assuming a ΛCDM cosmology with $\Omega_{\rm M}$=0.27, Ω_Λ=0.73 and a Hubble constant of H_0=71 km s^{-1} Mpc^{-1} using the luminosity distances given by Hogg (1999). All errors are 1σ unless stated otherwise.

2. Observations and data reduction

GRB 050603 was detected by the BAT on 2005-June-03 at 06:29:05 UT (Retter et al. 2005) with the trigger ID 131560. Due to engineering tests of the *Swift* satellite, the narrow-field instruments, UVOT and XRT, were unable to observe the GRB afterglow until about 9.5 and 11 hours after the burst, respectively.

The UVOT began observing at 15:42:59 UT (Brown et al. 2005a). The observations were made in the V filter with exposure time ratios of 1:8:1 per observing window so that the entire observation is not ruined if there is high background from the earth limb at the beginning or end of the observation. Only the middle exposures were used, to eliminate the problems of high background. The NASA *Swift* Data Center (SDC)-processed sky images were astrometrically aligned with respect to an image of the field from the Digitized Sky Survey. Aperture photometry was performed using a 6″ source aperture and a background annulus with inner and outer radii of 14″ and 30″ respectively. Once the afterglow in individual observations had fallen below 3σ above background they were co-added to bring the S/N ratio above a 3σ detection.

The GRB 050603 observations by the UVOT also revealed an infrequent problem in which the images do not contain events from the whole exposure time indicated in the header. Extension 4 of Sequence 00131560001 reported an exposure time of 1500s. However, a comparison of the count rate measured by the instrument and the counts in the image indicated that the image contained only 110 seconds of data. Thus only 7.3% of the data were actually recorded. This resulted in an erroneous magnitude being reported in Brown et al. (2005a), as pointed out by Berger (2005). We have corrected this by comparing the count rate as measured by the UVOT with the counts in the actual image to calculate the exposure time. When the header and calculated exposure times differed by more than 5%, the exposure keyword was changed to the calculated value. The software bug causing this problem was fixed on 2005-September-14 and data taken before that date will be checked and

corrected in the archive.

The XRT started to take data at 17:19:27 UT (Racusin et al. 2005). GRB050603 was observed over a period of about two weeks for a total of about 220 ks. The detailed observation log is listed in Table 1. All observations were performed in PC mode. The XRT data were reduced by the *xrtpipeline* software version 0.9.9. Source photons were selected by *XSELECT* in a circular region with a radius of r=47″ and the background photons in a circular region close by with a radius r=96″. For the spectral data events with grades 0-12 were selected with *XSELECT*. The spectral data were re-binned by *grppha* 3.0.0 having at least a minimum of 20 photons per bin. The spectra were analyzed by *XSPEC* version 11.3.2. The auxiliary response files were created by *xrtmkarf* and the standard response matrix swxpc0to12_20010101v007.rmf was used.

Background-subtracted X-ray light curves in the 0.3-10.0 keV energy range were constructed using the ESO Munich Image Data Analysis Software *MIDAS* (version 04Sep). The binning was dynamically performed. At the beginning of the observations the binning was set to 50 photons per bin while at later times it was reduced to 10 photons per bin as listed in Table 1. Also at later times the source extraction radius was reduced to 10 pixels (corresponding to r=23.6″) in order to avoid confusion by the background. The X-ray light curve was fitted by power law and broken power law models in *XSPEC*. The count rates were converted into an unabsorbed flux by an energy conversion factor (ECF) using a power law fit with the absorption column density fixed to the Galactic value (1.2×10^{20} cm^{-2}, Dickey & Lockman 1990). Only one ECF with ECF=3.76×10^{-11} ergs s^{-1} cm^{-2} count^{-1} was applied for the whole light curve. As shown below in §3.3.2, there is no obvious change of the spectral parameters between early and later observations.

3. Results

3.1. Positions

All positions given for GRB 050603 are listed in Table 2. Figure 1 displays the UVOT V-filter image of the GRB 050603 field with the BAT and XRT error circles superimposed as given in Table 2. The XRT position given in Table 2 is corrected for the XRT boresight offset (Moretti et al. 2005) and differs slightly from the positions given by Grupe et al. (2005) and Racusin et al. (2005). This new XRT position is in excellent agreement with the UVOT, optical, and radio positions (Brown et al. 2005a; Berger & McWilliam 2005; Cameron 2005).

3.2. BAT

The BAT mask-weighted light curve (Figure 2) shows three fast-rise-exponential-decay (FRED) like spikes with peaks at 2.7 and 0.85 s before the trigger and 0.15 s afterwards. Each spike had a width of 0.6 s FWHM. The left panel of Figure 2 displays the light curve of the whole 15-350 keV energy band. The right panel shows the light curve split into four energy bands: 15–25 keV, 25–50 keV, 50–100 keV, and 100–350 keV. The BAT light curve shows a harder spectrum during the spikes compared to the BAT observation after the spikes (Figure 3).

The time-averaged spectrum between T_0-3s and T_0+18s in the 15-150 keV band shown in Figure 4 is well fitted by a single power law with an energy spectral slope $\beta_\gamma = 0.17^{+0.07}_{-0.08}$ (χ^2/ν=51/57). The spectrum is background subtracted. It has the standard 80-channel BAT energy binning.

GRB 050603 had T_{90}=12±2s which classifies it as a long burst. The fluence in the observed 15–150 keV band was $(7.6\pm0.3)\times10^{-6}$ ergs cm^{-2}. Based on the redshift z=2.812 (Berger & Becker 2005), the k-corrected rest-frame 100–500 keV and 20 keV–2 MeV total isotropic equivalent energies $E_{\gamma,\rm iso}$=3.2×10^{53} ergs and $E_{\gamma,\rm iso}$=1.26×10^{54} ergs, respectively, are some of the largest measured among all GRBs detected by *Swift* (Nousek et al. 2006). The total energies are comparable to other high-energetic pre-*Swift* bursts such as GRB 990123 (Briggs et al. 1999; Corsi et al. 2005), GRB 000131 (Andersen et al. 2000), or GRB 010222 (in't Zand et al. 2001).

3.3. XRT data

3.3.1. XRT light curve

Figure 5 displays the 0.3-10 keV flux X-ray light curve of GRB 050603. The initial count rate at the beginning of the XRT observation was 0.06 counts s^{-1} which converts to a 0.3-10.0 keV unabsorbed flux $F_{\rm X} = 3\times10^{-12}$ ergs s^{-1} cm^{-2}. The 2.0-

10.0 keV unabsorbed flux was $F_{\rm X} = 2 \times 10^{-12}$ ergs s^{-1} cm^{-2}. The count rate was low enough that the data are not affected by pileup. The decay slope, derived from the 0.3-10.0 keV flux light curve shown in Figure 5, is unusually steep with $\alpha = 1.76^{+0.15}_{-0.07}$. This makes GRB 050603 a relatively rapidly fading afterglow in its late phase (Nousek et al. 2006). The data are consistent with one simple power law throughout the observation with a χ^2/ν=14.3/17.

Just before the detection of GRB 050603 the XRT MOS CCD was hit by a micro-meteorite which caused severe damage to columns 294 and 320. These columns (and several adjacent ones) have been disabled on-board and are not useable. If the PSF of a source overlaps these bad columns, the measured flux can be incorrect. Since the source position on the detector changes with each orbit, this can lead to errors in the light curve. We have verified that the GRB was not positioned on the bad columns during this observation.

3.3.2. X-ray spectral analysis

Table 3 lists the results of the spectral analysis of the XRT data. A simple power law model with Galactic absorption fits the spectra well for the segments 001 and 002 (Table 1) data, resulting in X-ray energy spectral slopes $\beta_{\rm X}$=0.80±0.17 and 0.62±0.13 for segments 001 and 002, respectively. The simultaneous fit to the segment 001 and 002 data is shown in Figure 6. The energy ranges of the two spectra are different due to the S/N and teh binning of the channels using *grppha*. This fits results in an X-ray spectra slope $\beta_{\rm X}$=0.71±0.10. In all cases, no additional intrinsic absorption is required. Leaving the absorption column density as a free parameter results in an absorption column density which is significantly below the Galactic value. As shown in Figure 6 there are some apparent residuals around 0.5 and 2.0 keV. These features are due to systematic errors in the still ongoing calibration of the auxiliary response file (see the XRT calibration document XRT-OAB-CAL-ARF-v3[1] and Romano et al. 2005).

[1]The calibration document XRT-OAB-CAL-ARF-v3 can be found under: http://swift.gsfc.nasa.gov/docs/heasarc/caldb/swift/docs/xrt/index.html

3.4. UVOT

The V magnitudes for GRB 050603 are listed in Table 4 and the V-band light curve is shown in Figure 7. The first measurement, V=18.2 at 9.5 hours after the burst, is brighter than any other optical *Swift* afterglow at the same time, many of which are not optically detected at all (see e.g. Roming et al. 2005b), and is among the brightest of all optical afterglows with the exception of GRB 030329 (see e.g. Berger et al. 2005). The X-ray and optical decay slopes are similar, with the UVOT points decaying with a power law slope of 1.8±0.2 with χ^2/ν=18/7. There is no indication of a break near 12 hours as suggested by Berger & Becker (2005), though the errors and wide temporal sampling do not allow a definitive statement. The steepness of the decay indicates that the break may have already occurred before our observations began, which would put a putative break at less than T+9 hours post-burst.

The large value of χ^2/ν indicates that the deviations from the simple power law may be real, though the largest deviations are only 2 σ. Li et al. (2006), in an independent analysis of the UVOT data, also concluded that this afterglow exhibited real fluctuations from a powerlaw decay. The power law decay reported by Li et al. (2006) is 1.86±0.06, which is consistent with our results and also in agreement with that seen in the X-rays.

3.5. Other wavelengths

GRB 050603 was the target of several ground-based observations at radio and optical wavelengths. Cameron (2005) reported the Very Large Array (VLA) position at 8.46 GHz as listed in Table 2. The flux density was 262±41 μJy at 8.4 hours after the burst. The afterglow was also observed by SCUBA at 450 and 850 μm at 11.2 and 13.3 hours after the burst, respectively. Barnard et al. (2005) reported of a 1.2σ detection with a flux density of 2.408±1.973 mJy at 450 μm, but no detection at 850μm.

Berger & McWilliam (2005) reported an R-band detection of the afterglow with the 2.5m du Pont telescope at Las Campanas Observatory 3.4 hours after the burst with R=16.5 mag. The optical position is given in Table 2. Berger & Becker (2005) measured the redshift of the afterglow as z=2.821 based on a single emission line which was

interpreted as Lyα. This observation was performed with the Magellan/Baade telescope 2.13 days after the burst.

GRB 050603 was also detected by the IBIS instrument on board INTEGRAL in the 40-300 keV energy range (Gotz & Mereghetti 2005). However, because the burst was outside the field of view it could not be localized. The duration of the burst seen by IBIS agreed with the results from the BAT. Golenetskii et al. (2005) reported the detection of GRB050603 by Konus-Wind in the observed 20keV-3MeV range. Its fluence in this energy band was $(3.41 \pm 0.06) \times 10^{-5}$ ergs cm^{-2} with a duration of 6 s and an observed $E_{\rm peak}$=349±28 keV.

4. Discussion

GRB 050603 was a particularly bright and energetic burst. The 15-150 keV fluence of 7.6× 10^{-6} ergs cm^{-2} places it among the top 10% of *Swift* bursts. The isotropic energy of 1.26×10^{54} ergs makes it one of the most energetic bursts ever detected. Combined with the rest-frame $E_{\rm peak}$=1.3 MeV, GRB 050603 is consistent with the Amati relation (Amati et al. 2002).

With an optical magnitude of V=18.2 9.5 hours after the burst it was also the brightest optical afterglow seen so far by *Swift* at this late time after the burst. The only burst that had a comparable magnitude (V=18.9) at 10 hours after the burst was GRB 050525 (Blustin et al. 2006). All other bursts were far below this magnitude at this time after the burst. In X-rays, however, the afterglow of GRB 050603 was not the brightest one among other *Swift* bursts observed at similar times after the trigger.

The X-ray afterglow of GRB 050603 decayed with a rather steep slope of α=1.76±0.07, compared with the mean decay slope of $\alpha = 1.34\pm0.32$ for 27 bursts listed in Nousek et al. (2006). This is intermediate between the slopes of $\sim 1.3 \pm 0.1$ obtained from Chandra grating observations, XMM observations, and Beppo-SAX afterglows discussed in Gendre et al. (2006), but is somewhat shallower than the mean decay slope of $\alpha_{\rm X}$=2.0±0.3 from their survey of Chandra imaging afterglow observations. It is also intermediate between the expectations for the "normal" afterglow slope following the end of energy injection by the central engine, and the steeper slope expected following the end of energy injection by the central engine. We note, however, that the decay slope in the V-band filter ($\alpha = 1.8 \pm 0.2$) is consistent with the X-ray decay slope, consistent with the typical signature of an afterglow after the jet break (Sari et al. 1999). This suggests the possibility that GRB 050603 had an early jet break before 2.9 hours (rest-frame) after the burst. If we assume that the jet break happened before the start of the UVOT and XRT observations, we can use the dependence of jet angle on break time (Sari et al. 1999; Frail et al. 2001) to place a limit on the jet opening angle of $\Theta_j < 1.^\circ3$, where we have used $E_{\rm iso} = 1.26\times10^{54}$ ergs and we assumed the density of the circum-burst matter is 0.1 cm^{-3}. We note that Bloom, Frail, & Kulkarni (2003) argue for a larger typical circum-burst density of 10 cm^{-3}, which would imply a slightly larger jet angle limit of $2.^\circ3$.

In order to check the jet interpretation, we compare the observed $\alpha_{\rm X}=1.76^{+0.15}_{-0.07}$ and $\beta_{\rm X}$=0.71±0.10 to the prediction of the jet model. For the familiar case of $p > 2$ (where p is the electron spectral index), one requires that $\alpha_{\rm X} - 2\beta_{\rm X} = 0$ ($\nu > \nu_c$) or $\alpha_{\rm X} - 2\beta_{\rm X} = 1$ ($\nu_m < \nu < \nu_c$), where ν_m is the typical synchrotron frequency (injection frequency) and ν_c is the cooling frequency (Rhoads 1999). In this case, we have $\alpha_{\rm X} - 2\beta_{\rm X} = 0.34^{+0.18}_{-0.12}$. Both cases are inconsistent with the data at the $> 2.8\sigma$ level. We therefore consider the case of $1 < p < 2$ (Dai & Cheng 2001). For $\nu > \nu_c$, this case has $2\alpha_{\rm X} - \beta_{\rm X} = 3$, while the data have $2\alpha_{\rm X} - \beta_{\rm X} = 2.81^{+0.32}_{-0.12}$, in good agreement with theory. In this regime the electron index is $p = 2\beta_{\rm X} = 1.4 \pm 0.2$. This case also has $\alpha_{\rm O} = \alpha_{\rm X}$ as long as the self-absorption frequency is below the optical band, in agreement with the observations. In this case, we expect $\beta_{\rm O} = \beta_{\rm X}$ if the optical band is above the cooling frequency, or $\beta_{\rm O} = 0.2 \pm 0.1$ if the optical band is between the injection frequency and the cooling frequency; however, with only V-band data we cannot constrain $\beta_{\rm O}$ directly. The observed spectral index between the X-ray and optical bands is $\beta_{\rm OX}$[2]=0.04. These spectral slopes suggest that there is a break in the spectrum between the optical and X-rays

[2]Here we define the optical to X-ray spectral slope $\beta_{\rm OX} = log(5460\mathring{A} \times f_{5460\mathring{A}}) - log(1{\rm keV} \times f_{1{\rm KeV}})$

suggesting that the optical band is between the injection and cooling frequencies. We therefore conclude that the jet interpretation fits these data provided there is a flat electron energy spectrum $p = 1.4$ (Dai & Cheng 2001). We note however, that this interpretation is at odds with the expectations from Liang & Zhang (2005) who find the relation $E_{\gamma,iso,52} = 0.85 \times (\frac{E_{\rm peak}}{100\ {\rm keV}})^{1.94} \times t^{-1.34}$, which predicts a jet break in the optical light curve at 1 day after the burst in the rest-frame, or 3.8 days in the observed frame.

We would like to thank the anonymous referee for valuable comments and suggestions that improved the paper. We would also like to thank Vicki Barnard and Brian Cameron for their information on the SCUBA and VLA observations. We made use of data obtained through the High Energy Astrophysics Science Archive Research Center Online Service, provided by the NASA/Goddard Space Flight Center. This work has been supported by NASA contract NAS5-00136, SAO grant GO5-6076 BASIC and NASA grant NNG05GF43G.

REFERENCES

Amati, L., Frontera, F., Tavani, M., et al., 2002, A&A, 390, 81

Andersen, M.I., et al., 2000, A&A, 364, L54

Barnard, V., Schieven, G., Tilanus, R., Lundin, E., & Ivison, R., 2005, GCN 3515

Barthelmy, S.D., 2005, Space Science Reviews, 120, 143

Berger, E., & McWilliam, A., 2005, GCN 3511

Berger, E., & Becker, G., 2005, GCN 3520

Berger, E., et al., 2005, ApJ, 629, 328

Bloom, J. S., Frail, D. A., & Kulkarni, S. R. 2003, ApJ, 594, 674

Blustin, A.J., et al., 2006, ApJ, 637, 901

Briggs, M.S., et al., 1999, ApJ, 524, 82

Brown, P., et al., 2005a, GCN 3516

Brown, P., et al., 2005b, GCN 3549

Burrows, D.N., Hill, J.E., Chincarini, G., et al., 2005a, ApJ, 622, L85

Burrows, D.N., et al., 2005b, Space Science Reviews, 120, 165

Cameron, P.B., 2005, GCN 3513

Corsi, A., et al., 2005, A&A, 438, 829

Dai, Z.G., & Cheng, K.S., 2001, ApJ, 558, L109

Dickey, J.M., & Lockman, F.J., 1990, ARA&A, 28, 215

Eichler, D., Livio, M., Piran, T., & Schramm, D.N., 1989, Nature, 340, 126

Fenimore, E., et al., 2005, GCN 3512

Frail, D.A., Kulkarni, S.R., Sari, R., et al., 2001, ApJ, 562, L55

Gehrels, N., et al., 2004, ApJ, 611, 1005

Gendre, B., & Boër, M., 2005, A&A, 430, 465

Gendre, B., Corsi, A., & Piro, L., 2006, A&A, in press, astro-ph/0507710

Golenetskii, S., Aptekar, R., Mazets, E., Pal'shin, V., Frederiks, D., & Cline, T., 2005, GCN 3518

Gotz, D., & Mereghetti, S., 2005, GCN 3510

Grupe, D., Retter, A., Burrows, D.N., Kennea, J.A., & Gehrels, N., 2005, GCN 3519

Hill, J.E., et al., 2004, SPIE, 5165, 217

Hogg, D., 1999, astro-ph/9905116

in't Zand, J.J.M., et al., 2001, ApJ, 559, 710

Kouveliotou, C., et al., 1993, ApJ, 541, L101

Li, W., Jha, S., Filippenko, A.V., Bloom, J.S., Pooley, D., Foley, J., & Perley, D.A., 2006, PASP, 118, 37

Liang, E., & Zhang, B., 2005, ApJ, 633, 611

Mason, K.O., et al., 2001, A&A, 365, L36

Mészáros , P., & Rees, M. J. 1997, ApJ, 476, 232

Moretti, A., et al., 2005, ApJ, submitted, astro-ph/0511604

Nousek, J., Kouveliotou, C., Grupe, D., Page, K.L., et al., 2006, ApJ, in press, astro/ph-0508332

Paczyński, B., 1991, Acta Astron., 41, 257

Racusin, J.L., Burrows, D.N., Kennea, J.A., Retter, A., Pagani, C., Wells, A., & Gehrels, N., 2005, GCN 3514

Retter, A., Parsons, A., Gehrels, N., Gronwall, C., Markwardt, C.B., & Palmer, D., 2005, GCN 3509

Rhoads, J., 1999, ApJ, 525, 737

Romano, P., et al., 2005, SPIE, 5898, 369

Roming, P.W.A., et al., 2005, Space Science Reviews, 120, 95

Roming, P.W.A., et al., 2005b, ApJ submitted, astro-ph/0509273

Sari, R., Piran, T., & Narayan, R., 1998, ApJ, 497, L17

Sari, R., Piran, T., & Halpern, J.P., 1999, ApJ, 519, L17

Turner, M.J.L., Abbey, A., Arnaud, M., et al., 2001, A&A, 365, L27

Woosley, S.E., 1993, ApJ, 405, 273

Zhang, B., & Mészáros , P., 2004, Int. Journal of Modern Physics A, Vol. 19, No. 15, 2385

Zhang, B., Fan, Y.Z., Dyks, J., Kobayashi, S., Mészáros , P., Burrows, B.N., Nousek, J.A., & Gehrels, N., 2006, ApJ, submitted, astro-ph/0508321

This 2-column preprint was prepared with the AAS LaTeX macros v5.2.

TABLE 1
LOG OF OF THE *Swift* XRT OBSERVATIONS OF GRB 050603

Segment	T-start[1]	T-stop[1]	T_{exp}[2]	Binning[3]
001	2005-06-03 15:49:47	2005-06-03 22:32:14	7122	50
002	2005-06-04 00:02:16	2005-06-06 21:10:00	72838	50
003	2005-06-07 00:04:50	2005-06-07 23:15:57	14612	25
004	2005-06-08 00:26:48	2005-06-08 23:22:58	11858	15
005	2005-06-09 00:32:42	2005-06-09 23:28:58	9840	10
006	2005-06-10 00:39:43	2005-06-10 23:35:57	11184	10
007	2005-06-11 00:55:38	2005-06-11 22:05:57	6463	ul[4]
008	2005-06-14 20:23:42	2005-06-14 23:59:56	3766	ul[4]
009	2005-06-15 00:58:31	2005-06-15 23:59:59	16453	ul[4]
010	2005-06-16 00:04:59	2005-06-16 23:59:57	11475	ul[4]
011	2005-06-17 01:18:43	2005-06-17 06:39:57	6292	ul[4]
012	2005-06-18 00:05:01	2005-06-20 23:03:20	44626	ul[4]
013	2005-06-24 00:28:17	2005-06-24 02:35:53	3284	ul[4]

[1]Start and End times are given in UT

[2]Observing time given in s

[3]Number of photons per bin in the light curve

[4]The source is not detected and only an upper limit can be given.

TABLE 2
CALCULATED POSITIONS OF GRB050603. BAT1 AND BAT2 REFER TO THE POSITIONS AS SHOWN IN FIGURE 1.

Position from	RA (J2000)	Dec (J2000)	Position error[1]	reference
BAT on-board (BAT1)	02 39 55	–25 10 57	240	Retter et al. (2005)
BAT ground (BAT2)	02 39 56	–25 11 41	60	Fenimore et al. (2005)
XRT	02 39 56.73	–25 10 54.36	3.9	Moretti et al. (2005)
UVOT V-filter	02 39 56.8	–25 10 54.9	1.0	Brown et al. (2005a)
Las Campanas R-band	02 39 57	–25 10 54	0.5	Berger & McWilliam (2005)
VLA 8.5 GHz	02 39 56.9	–25 10 54.6	0.1	Cameron (2005)

[1]Position uncertainty is given in arc seconds

TABLE 3

SPECTRAL ANALYSIS OF GRB 050603 WITH A POWER LAW FIT WITH THE COLUMN DENSITY FIXED AT THE GALACTIC VALUE (1.19×10^{20} CM^{-2}, DICKEY & LOCKMAN 1990)

Segment	β_X	χ^2/ν
001	0.80±0.17	13.5/13
002	0.62±0.13	24.3/22
001 + 002	0.71±0.10	39.2/36

TABLE 4

V-MAGNITUDES GRB 050603 FROM THE UVOT OBSERVATIONS

$T_{\rm after\ burst}$[1]	$T_{\rm exp}$[2]	V mag	V error
34093	1298	18.19	0.08
39276	110	18.73	0.40
45864	1772	19.47	0.21
51840	2104	19.33	0.17
57096	1200	19.02	0.17
63900	1205	19.67	0.33
75024	2056	20.1	0.37
129996	10458	21.06	0.37
219708	10945	21.48	0.36

[1]The times after the burst are given in s and mark the middle of the time bin.

[2]Exposure times $T_{\rm exp}$ given in s.

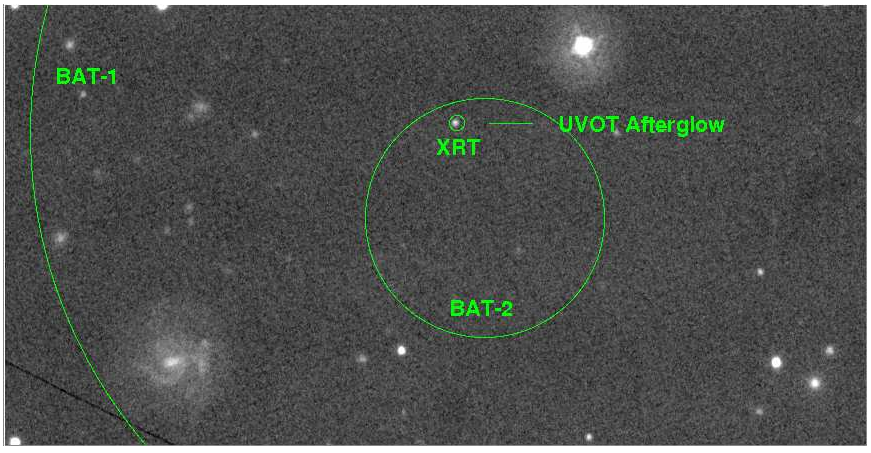

Fig. 1.— *Swift* UVOT V-filter image of the field around GRB 050603 with the BAT and XRT error circles superimposed. Positions are given in Table 2. BAT-1 refers to the onboard processed position and error circle and BAT-2 to the error circle from the data processed on the ground.

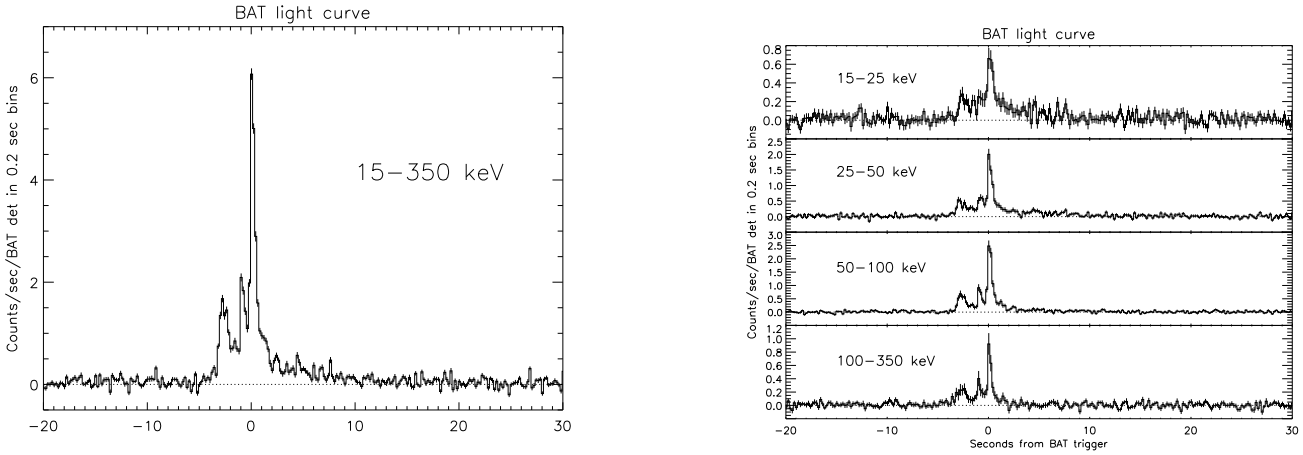

Fig. 2.— *Swift* BAT light curves, left panel shows the light curve in the energy range 15-350 keV, and the right panel the light curve split into 4 subranges (see text).

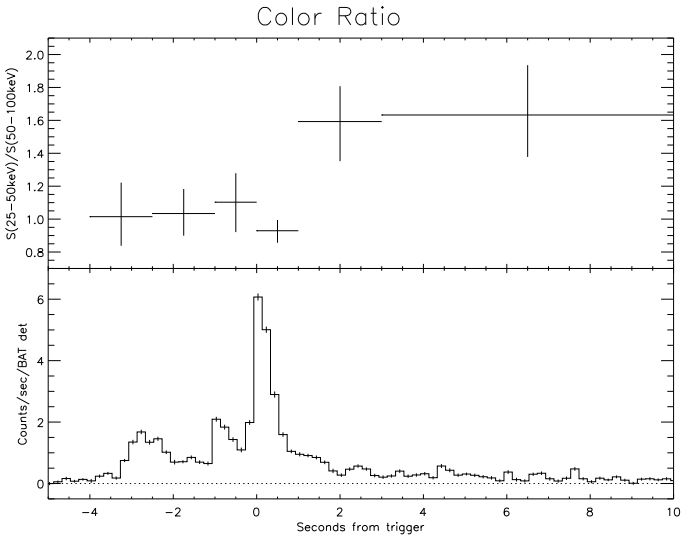

Fig. 3.— *Swift* BAT color ratio (top) and light curve (bottom).

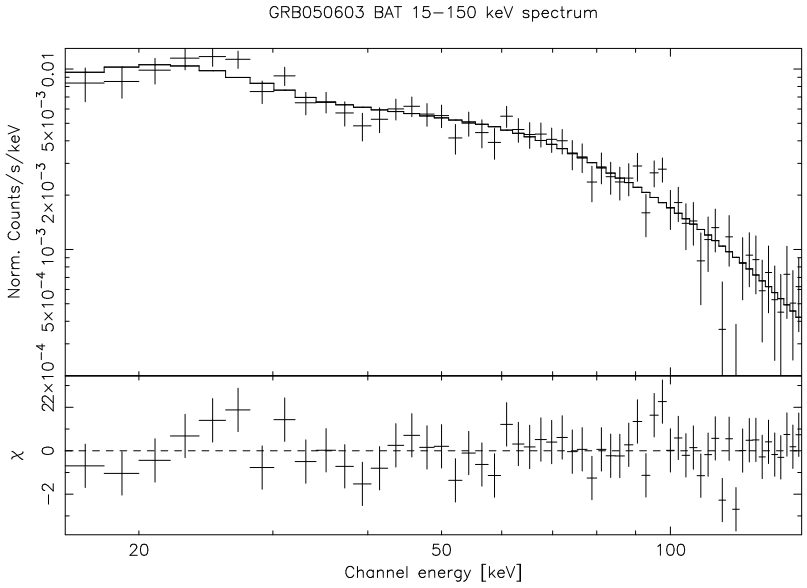

Fig. 4.— *Swift* BAT 15-150 keV spectrum

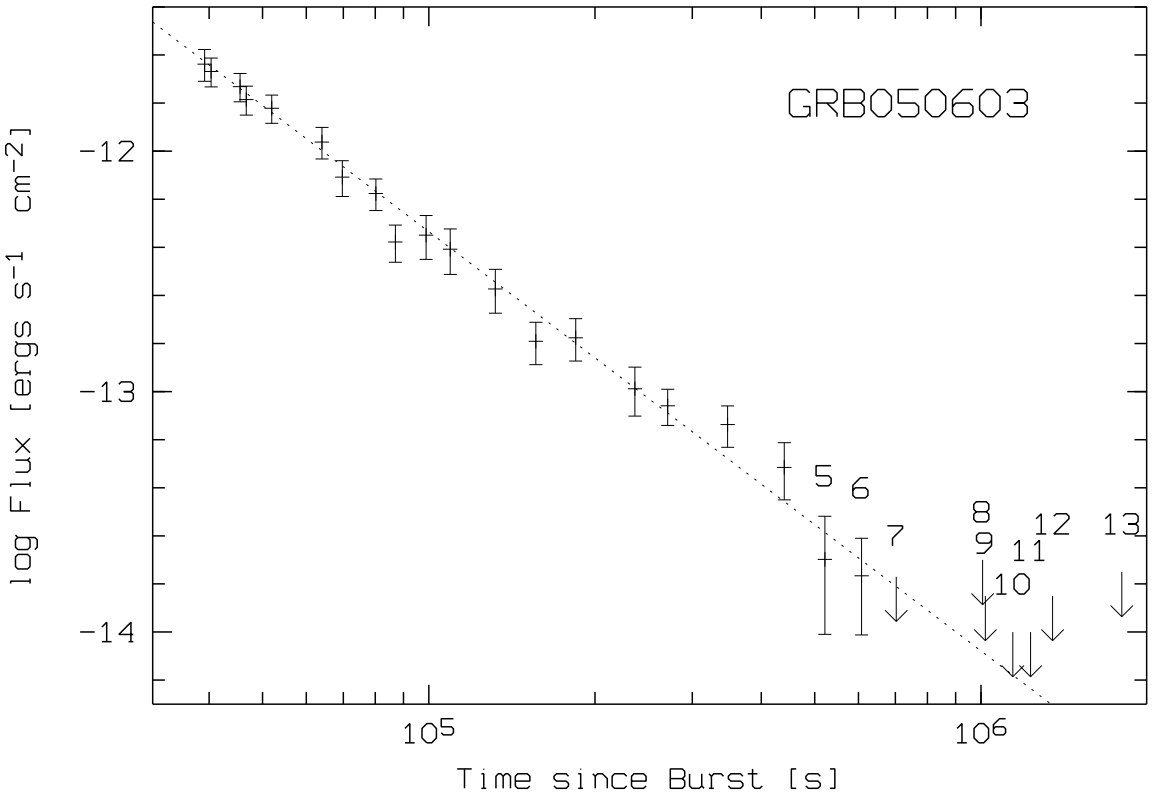

Fig. 5.— *Swift* XRT 0.3-10.0 keV unabsorbed flux light curve of GRB 050603 fitted in XSPEC by a single power law with α_3=1.76±0.07. The downwards arrows represent 3σ upper limits. The Numbers 5-13 refer to the segments as given in Table 1.

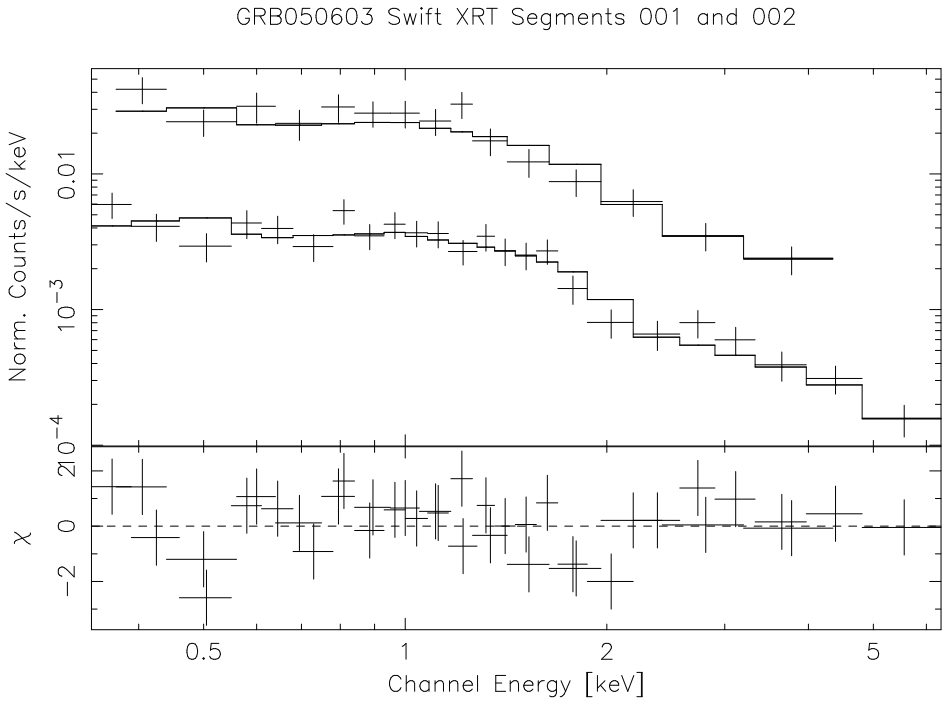

Fig. 6.— X-ray spectra of the observation segments 001 (top) and 002 (Table 1 of GRB 050603 fitted by a single power law (see Table 3). The residuals at 0.5 and 2 keV are caused by systematic errors in the auxiliary response file calibration (§3.3.2).

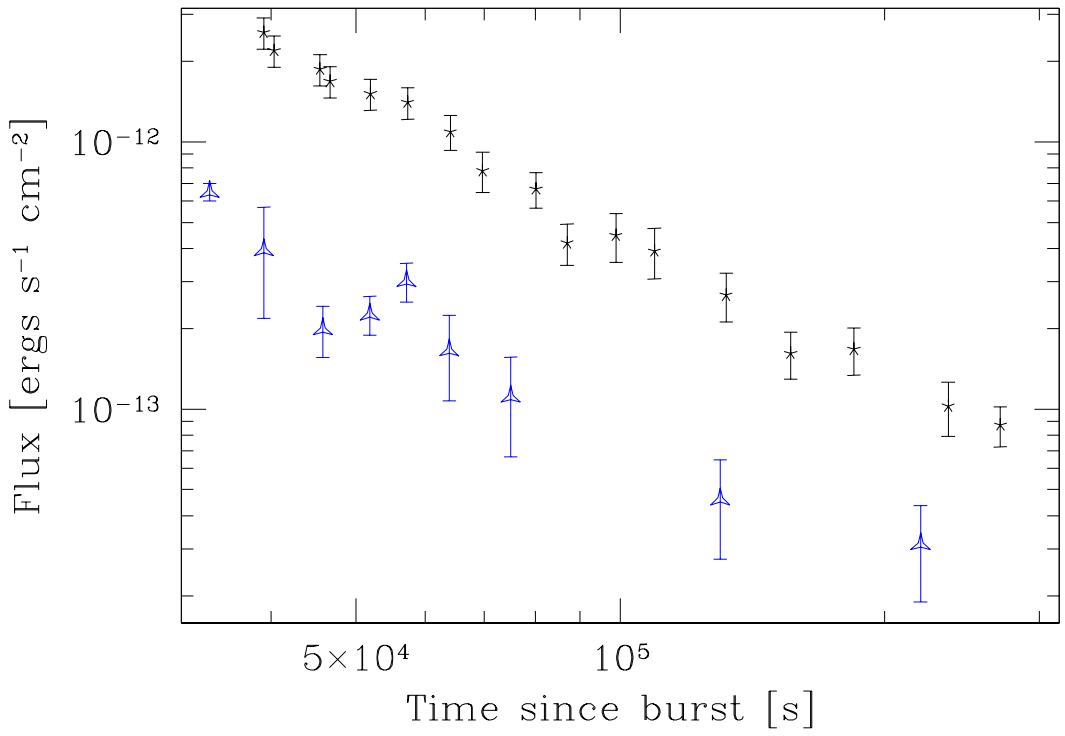

Fig. 7.— Combined XRT and UVOT V-filter light curves. The UVOT V fluxes were multiplied by a factor of 10^6 in order to plot them together with the XRT data. The XRT data are displayed as crosses and the UVOT V-band data as triangles.